

# The Composition Pulling Effect in MOVPE Grown InGaN on GaN and AlGaN and its TEM Characterization

K. Hiramatsu  
Mie University

Y. Kawaguchi, M. Shimizu, N. Sawaki  
Nagoya University

T. Zheleva, Robert F. Davis  
North Carolina State University

H. Tsuda, W. Taki, N. Kuwano, K. Oki  
Kyushu University

This *invited* article was received on March 25, 1997 and accepted on May 13, 1997.

## Abstract

InGaN films have been grown on GaN and AlGaN epitaxial layers by metalorganic vapor phase epitaxy. The "composition pulling effect" during the initial InGaN growth stages has been studied as a function of the lattice mismatch between the InGaN and the underlying epitaxial layer. The crystalline quality of the InGaN is good near the InGaN/GaN interface and the composition is close to that of GaN. However, with increasing InGaN film thickness, the crystal quality deteriorates and the indium mole fraction increases. The composition pulling effect becomes stronger with increasing lattice mismatch. It is suggested that indium atoms are excluded from the InGaN lattice during the early growth stages to reduce the deformation energy from the lattice mismatch. TEM observations of the InGaN/GaN structure reveal that the degradation of the crystalline quality of InGaN films grown on GaN is caused by pit formation which arises from edge dislocations propagating through the InGaN film from the underlying GaN.

## 1. Introduction

High brightness III-V nitride semiconductor blue and green light-emitting diodes (LEDs) have been already put to practical use [1][2]. Recently, the realization of short wavelength laser diodes (LDs) has been reported [3][4]. These optoelectronic devices consist of double heterostructures (DH) which include an InGaN active layer sandwiched between GaN and AlGaN cladding layers. As a result, the large lattice mismatch between InGaN/GaN or InGaN/AlGaN could conceivably have a great influence on the crystal growth mechanisms of InGaN and its performance in the device.

In our previous paper [5] we reported a "composition pulling effect" in InGaN films. We observed that the indium mole fraction is low during the initial stages of InGaN growth on GaN epilayers, and the mole fraction increases with increasing film thickness. We suggested that this effect is related to the strain of the lattice mismatched InGaN/GaN system. The composition pulling effect is known in other systems, such as LPE-grown InGaP/GaAs and InGaP/GaAsP [6] and MBE-grown InAlAs/InP [7].

In this paper we report InGaN/GaN and InGaN/AlGaN heterostructures fabricated to investigate the composition pulling effect as a function of lattice mismatch. For comparison with these heterostructures, we grew InGaN directly on low temperature (LT) buffer layers in which the lattice strain was relaxed. Furthermore, the crystalline microstructure of InGaN/GaN was studied by TEM.

## 2. Experiment

Crystal growth of InGaN and other III-V nitride semiconductors was accomplished using a vertical-type metalorganic vapor phase epitaxy (MOVPE) system at atmospheric pressure. C-plane sapphire ( $\alpha$ -Al<sub>2</sub>O<sub>3</sub>) was used as the substrate. Trimethylgallium (TMG), trimethylindium (TMI), trimethylaluminum (TMA) and ammonia (NH<sub>3</sub>) were used as Ga, In, Al and N sources, respectively. Hydrogen (H<sub>2</sub>) gas was used as the carrier gas during the growth process.

The substrate was heated to 1150°C in a stream of H<sub>2</sub> for 10 min to thermally clean the substrate. Then, two types of heterostructures were fabricated: (1) InGaN grown on a GaN or AlGa<sub>0.09</sub>N epitaxial layer and (2) InGaN grown directly on a LT buffer layer. Lattice deformation due to lattice mismatch between the hGa<sub>0.91</sub>N film and the underlying layer is present in (1), while it is relaxed by the LT buffer layer in (2). In case (1), the substrate temperature was lowered to 600°C to deposit the AlN LT buffer layer (50 nm). Next, the substrate temperature was elevated to 1050°C to grow a GaN or Al<sub>0.09</sub>Ga<sub>0.91</sub>N epitaxial layer (~2.5 μm thick). Next, the substrate temperature was lowered to grow InGaN. In case (2), the substrate temperature was lowered to 600°C to deposit the AlN, GaN or AlGa<sub>0.09</sub>N LT buffer layer (about 50 nm). The substrate temperature was then elevated to 1050°C for a few seconds thermal anneal, then immediately lowered to grow the InGaN film.

To change the lattice mismatch between the InGaN film and the underlying epitaxial layer, the indium mole fraction of the InGaN was changed by controlling the growth temperature ( $T_g = 800^\circ\text{C}$  and  $840^\circ\text{C}$ ) and by using different underlying epitaxial layers of GaN and Al<sub>0.09</sub>Ga<sub>0.91</sub>N. During the InGaN growth, the flow rate of NH<sub>3</sub>, TMG and TMI were maintained at 4.0 l/min, 7.33 μmol/min and 18.7 μmol/min, respectively. Details of the growth conditions and growth processes are described in [5].

The indium mole fraction of the InGaN films was determined by Electron Probe Microanalysis (EPMA). Photoluminescence (PL) measurements were carried out at room temperature (RT) using a He-Cd laser (325 nm). Cross-sectional TEM images of crystalline InGaN/GaN microstructures were also made.

## 3. Results and Discussion

### 3.1. Observation by SEM

Figure 1 shows a cross-sectional SEM image of InGaN grown directly on an AlN LT buffer layer at  $T_g = 800^\circ\text{C}$  (case (2)). The indium mole fraction was determined to be 0.20 by EPMA. The surface is smooth and uniform InGaN growth is obtained.

Figure 2 shows surface and cross-sectional SEM images of InGaN grown on a GaN epitaxial layer at  $T_g = 800^\circ\text{C}$  (case (1)) for different growth times of 5 min, 10 min, 15 min and 60 min. Defects begin to appear on the surface at the InGaN film thickness of 0.2 μm (Figure 2 (a)). The surface gradually becomes rough (Figure 2 (b), Figure 2 (c)). The surface of InGaN grown for 60 min is very rough (Figure 2 (d)). As seen in Figure 2 (h), the InGaN film thickness was divided into two areas, a "homogeneous, layer type growth area" and a "rough, columnar type growth area".

### 3.2. PL Measurement

Figure 3 shows the RT PL spectra of InGaN films grown directly on the AlN buffer layer at  $T_g = 800^\circ\text{C}$  for growth times of 15 min, 30 min and 60 min (thicknesses of 0.5 μm to 2 μm). The InGaN band-edge-emissions were constant at 420 nm. The PL peak wavelength did not change when InGaN films were grown on other LT buffer layers (GaN and AlGa<sub>0.09</sub>N).

Figure 4 shows RT PL spectra of InGaN films grown on a GaN epitaxial layer at  $T_g = 800^\circ\text{C}$ . The thinnest InGaN film has a sharp PL spectrum at a peak wavelength of 387 nm, and its indium mole fraction is 0.07 as measured from EPMA. As the InGaN thickness increases, the peak wavelength shifts toward longer wavelengths, eventually becoming constant at 420 nm. The indium mole fraction determined by EPMA increased from 0.07 to 0.2, corresponding to the red shift of the PL peak wavelength.

Figure 5 shows the dependence of the InGaN PL peak wavelength on the InGaN film thickness for various InGaN film growth conditions: InGaN films grown on a AlN LT buffer layer at  $T_g = 800^\circ\text{C}$  (a) and  $T_g = 840^\circ\text{C}$  (d), grown on a GaN epitaxial layer at  $T_g = 800^\circ\text{C}$  (b) and  $T_g = 840^\circ\text{C}$  (c), and grown on an Al<sub>0.09</sub>Ga<sub>0.91</sub>N epitaxial layer at  $T_g = 800^\circ\text{C}$  (e) and  $T_g = 840^\circ\text{C}$  (f).

GaN epitaxial layer at  $T_g = 800^\circ\text{C}$  (b) and  $T_g = 840^\circ\text{C}$  (e), and grown on an  $\text{Al}_{0.09}\text{Ga}_{0.91}\text{N}$  epitaxial layer at  $T_g = 800^\circ\text{C}$  (c). Here, we can consider three different lattice mismatches between InGaN and underlying epitaxial layers ((b), (e) and (c)). The InGaN grown directly on the LT buffer layer maintained a thickness independent peak PL wavelength 420 nm for  $800^\circ\text{C}$  growth (a) and 383 nm for  $840^\circ\text{C}$  growth (d) suggesting that the composition is unaffected by the interface and is given simply by the thermal equilibrium between the gas phase and solid phase. The composition pulling effect does not occur in this case.

On the other hand, thin InGaN grown at  $800^\circ\text{C}$  on GaN (b) and  $\text{Al}_{0.09}\text{Ga}_{0.91}\text{N}$  (c) epitaxial layers initially has a shorter wavelength than (a). With increasing film thickness, the PL peak wavelength shifts drastically toward longer wavelengths, finally reaching a constant value equal to (a). Furthermore, the thin InGaN films grown at  $840^\circ\text{C}$  on epitaxial GaN (e) have a shorter wavelength than (d), and with increasing the film thickness the InGaN PL peak wavelength shifts drastically toward longer wavelengths, finally becoming constant at a value equal to (d). The energy shift of the PL peak wavelength is  $>100$  meV. This value is much larger than the peak shift which could be expected from lattice deformation which would be  $\sim 10$  meV [8]. Therefore, the peak shift is attributed to the compositional variation. The critical thickness at which the peak wavelength begins to switch corresponds to that at which the surface becomes rough, as seen in Figure 2. Figure 6 shows the composition pulling,  $\Delta x$ , in the initial growth stages of InGaN on GaN and AlGaIn epitaxial layers as a function of lattice mismatch  $\Delta a/a_b$  between the InGaN and underlying epitaxial layers. It is seen that with increasing the lattice mismatch, the composition pulling effect is enlarged.

It was found that the greater the lattice mismatch between InGaN and the underlying epitaxial layer was, a thinner the critical thickness and larger the compositional shift of InGaN resulted. Thus, the composition pulling effect is strongly affected by the lattice mismatch between InGaN and the underlying epitaxial layer. This implies that the indium distribution mechanism in InGaN is caused by the lattice deformation due to the lattice mismatch. That is, indium atoms are excluded from InGaN to reduce the deformation energy during the InGaN growth. This effect is similar to one which has been reported in the LPE growth of InGaP/GaAs and InGaP/GaAsP [6] and the MBE growth of InAlAs/InP [7].

### 3.3. Observation by TEM

To understand the degradation mechanism of the InGaN crystalline quality when grown on a GaN epitaxial layer, we observed cross-sectional TEM images of InGaN/GaN. Figure 7 shows a cross-sectional TEM image of InGaN film grown on GaN at  $800^\circ\text{C}$  for 5 min which reveals the whole thickness of the InGaN/GaN/AlN/ $\alpha$ - $\text{Al}_2\text{O}_3$  heterostructure. Although crystalline quality of the GaN epitaxial layer is quite good, there is a high density of threading dislocations penetrating the GaN layer along the c-axis from the AlN buffer layer to the InGaN/GaN interface. These dislocations are predominantly perfect edge dislocation with burgers vectors of the  $1/3\langle 11\bar{2}0 \rangle$  type [9].

Figure 8 (a) shows is a magnified TEM image of the InGaN/GaN interface, and Figure 8 (b) is a schematic diagram of that image. The threading dislocations penetrate into the InGaN layer and reach the InGaN surface where pits are formed. The pit has a hexagonal inverted pyramid-like structure. However, no other defects generate from the InGaN/GaN interface indicating that coherent InGaN growth occurs on the GaN layer at the early growth stages resulting in initially good crystal quality. The pits are clearly observed in the InGaN/GaN surface SEM image (Figure 2 (a)). The distribution of the pits corresponds to that of the dislocations penetrating the GaN layer. The pit pattern is similar to the dislocation pattern which has been observed by plan-view TEM of GaN on a LT buffer layer [9]. From the results of Ref. [9], it is suggested that the lines of pits are due to threading dislocations forming at grain boundaries in the GaN film. The calculated pit density is of the order of  $10^9 \text{ cm}^{-2}$ , which is in good agreement with the reported value of the dislocation density [9]. Thus it is found that the pits originate from edge dislocations penetrating the GaN layer.

Figure 9 shows cross-sectional images of InGaN grown on GaN at  $800^\circ\text{C}$  for 60 min. Figure 9 (a) is a TEM image near the InGaN/GaN interface, and Figure 9 (b) is a schematic diagram. Subsequent to pit formation in the initial growth stage of InGaN, the crystalline quality of InGaN deteriorates at the pit locations and these films have a large number of defects, including dislocations. Defect formation decreases the deformation energy stored in the InGaN layer owing to the lattice mismatch, and hence reduces the composition pulling effect. Consequently, the indium mole fraction is raised to a value that is determined by the thermal equilibrium between the gas phase and solid phase. Fringe contrast parallel to the facets is observed on the pits, which suggests that the change in the indium mole fraction occurs in those areas.

## 4. Conclusions

The "composition pulling effect" at the initial stages of InGaN grown on GaN and AlGaIn epitaxial layers by MOVPE

was investigated. The lattice mismatch between InGaN and the underlying epitaxial layer has a great influence on this effect. Indium atoms are excluded from the InGaN lattice to reduce the deformation energy due to the lattice mismatch during the InGaN growth. The composition pulling effect was weakened with increasing InGaN thickness because the lattice deformation is relaxed by the generation of a large number of crystalline defects. During InGaN growth, pits, attributed to edge dislocations propagating through from the GaN film, form on the surface. The crystal quality of further InGaN deteriorates at the pit locations causing thick InGaN films to have a large number of defects, including dislocations.

## Acknowledgments

This work was supported in part by Mitsubishi Cable Industries Ltd.

## References

- [1] Shuji Nakamura, Takashi Mukai, Masayuki Senoh, *Appl. Phys. Lett.* **64**, 1687-1689 (1994).
- [2] S. Nakamura, M. Senoh, N. Iwasa, S. Nagahama, T. Yamada, T. Mukai, *Jpn. J. Appl. Phys.* **34**, L1332-L1335 (1995).
- [3] S Nakamura, M Senoh, S Nagahama, N Iwasa, T Yamada, T Matsushita, H Kiyoku, Y Sugimoto, *Jpn. J. Appl. Phys.* **35**, L74-L76 (1996).
- [4] S. Nakamura, M. Senoh, S. Nagahama, N. Iwasa, T. Yamada, T. Matsushita, Y. Sugimoto, H. Kiyoku, *Appl. Phys. Lett.* **69**, 4056-4058 (1996).
- [5] M. Shimizu, Y. Kawaguchi, K. Hiramatsu, N. Sawaki, *Sol. St. Electr.* **41**, 145 (1997).
- [6] J. Ohta, M. Ishikawa, R. Itoh, N. Ogasawara, *Jpn. J. Appl. Phys.* **22**, L136 (1983).
- [7] M. Allovon, J. Primot, Y. Gao, M. Quillec, *J. Electron. Mater.* **18**, 505 (1989).
- [8] H. Amano, K. Hiramatsu, I. Akasaki, *Jpn. J. Appl. Phys.* **27**, L1384 (1988).
- [9] W. Qian, M. Skowronski, M. De Graef, K. Doverspike, L. B. Rowland, D. K. Gaskill, *Appl. Phys. Lett.* **66**, 1252-1254 (1995).

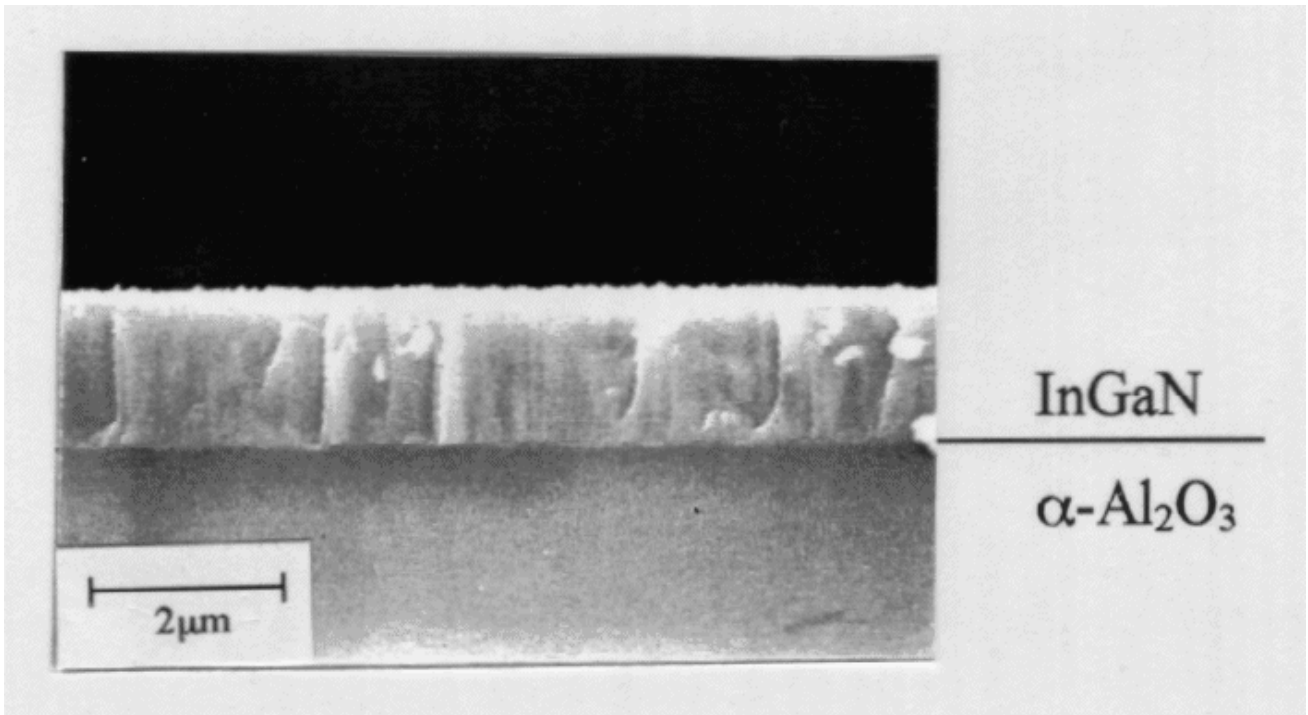


**Figure 1.** Cross-sectional SEM image of InGaN grown on the AlN LT buffer layer. InGaN were grown for 60 min.

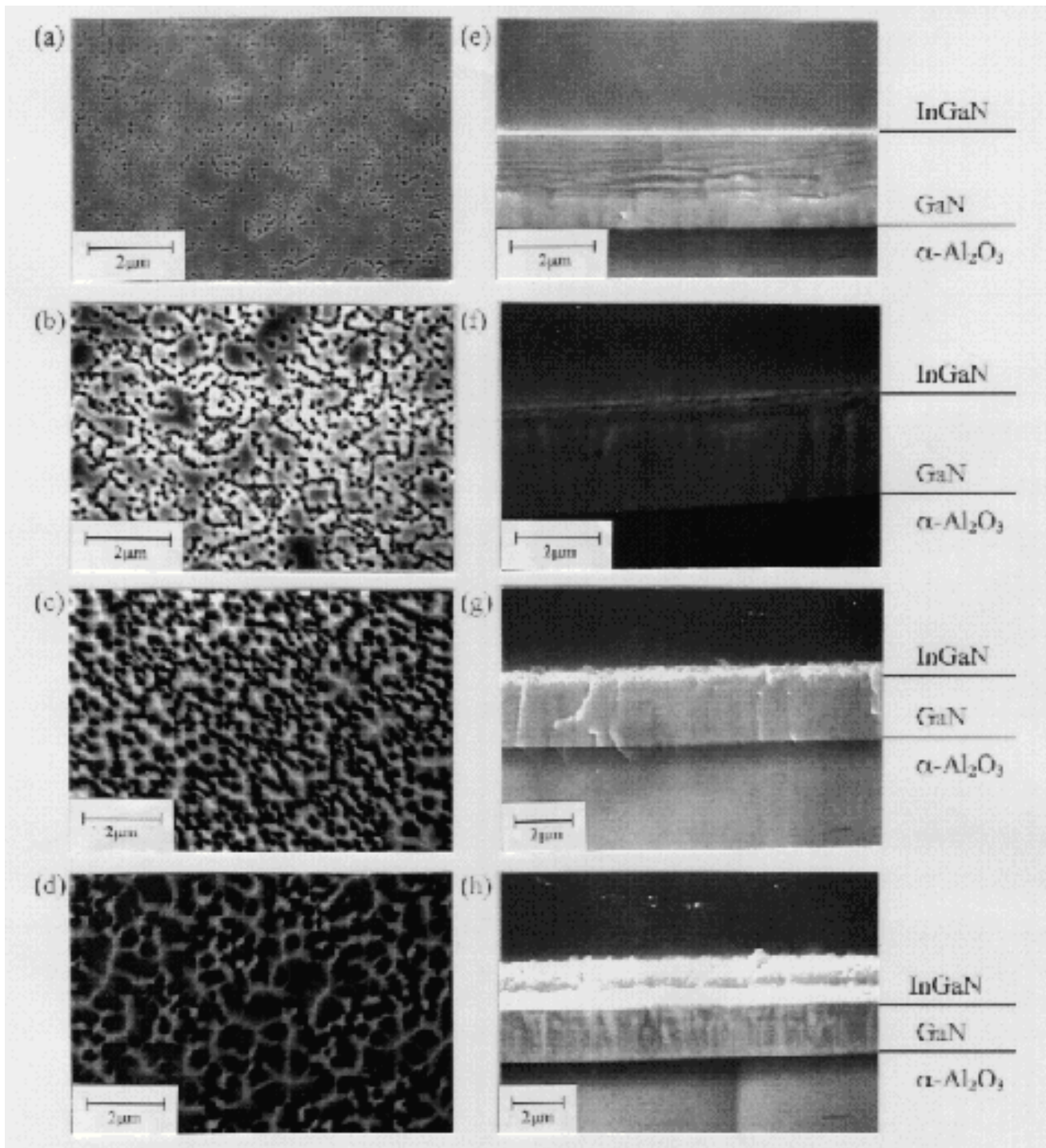


**Figure 2.** Surface ((a)-(d)) and cross-sectional ((e)-(h)) SEM images of InGaN grown on a GaN epitaxial layer at 800°C. InGaN layers were grown for (a),(e): 5 min, (b),(f): 10 min, (c),(g): 15 min and (d),(h): 60min.

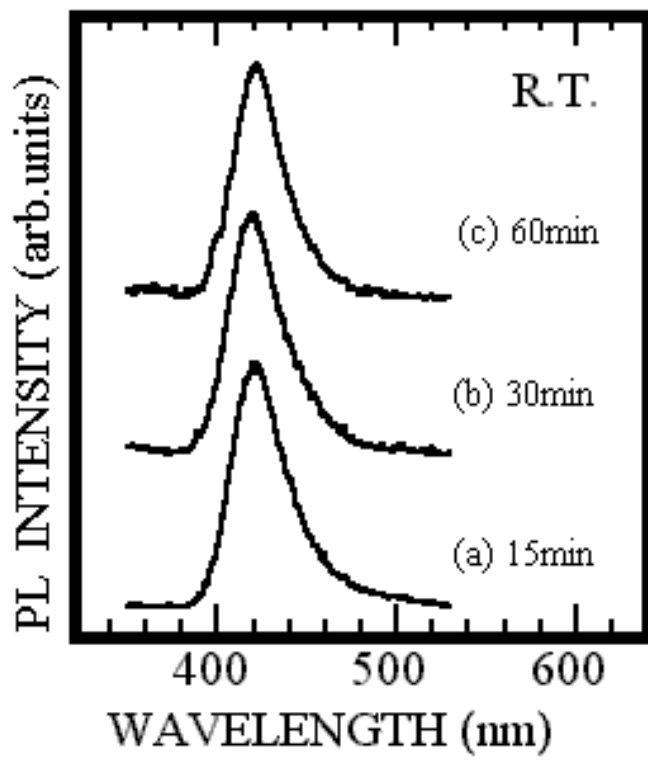


**Figure 3.** PL spectra at room temperature of InGaN grown on the AlN LT buffer layer. InGaN layers were grown for (a) 15 min, (b) 30 min and (c) 60 min.

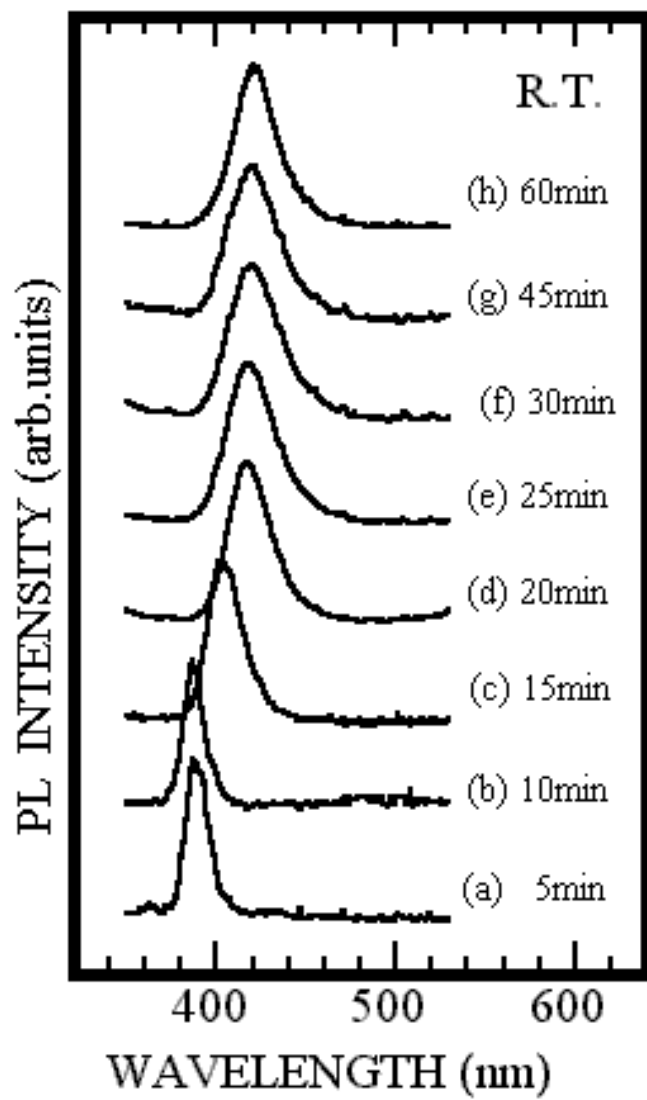


**Figure 4.** PL spectra at room temperature of InGaN grown on the GaN epitaxial layer. InGaN were grown for (a) 5 min, (b) 10 min, (c) 15 min, (d) 20 min, (e) 25 min, (f) 30 min, (g) 45 min and (h) 60 min.



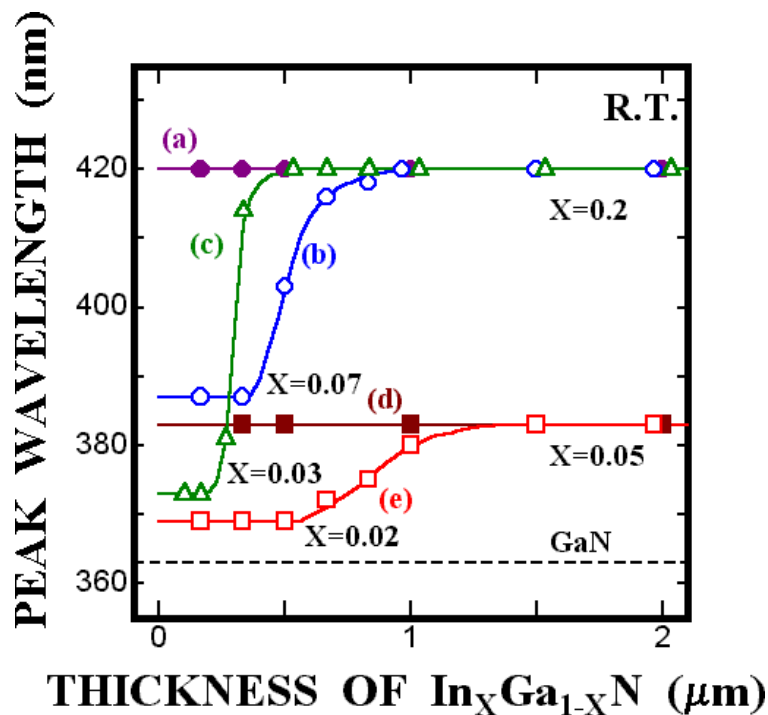


**Figure 5.** Growth thickness dependence of PL peak wavelength for InGaN. (a) InGaN on AlN LT buffer layer at  $T_g = 800^\circ\text{C}$ , (b) InGaN on GaN epitaxial layer at  $T_g = 800^\circ\text{C}$ , (c) InGaN on AlGaN epitaxial layer at  $T_g = 800^\circ\text{C}$ , (d) InGaN on AlN LT buffer layer at  $T_g = 840^\circ\text{C}$ , (e) InGaN on GaN epitaxial layer at  $T_g = 840^\circ\text{C}$ .

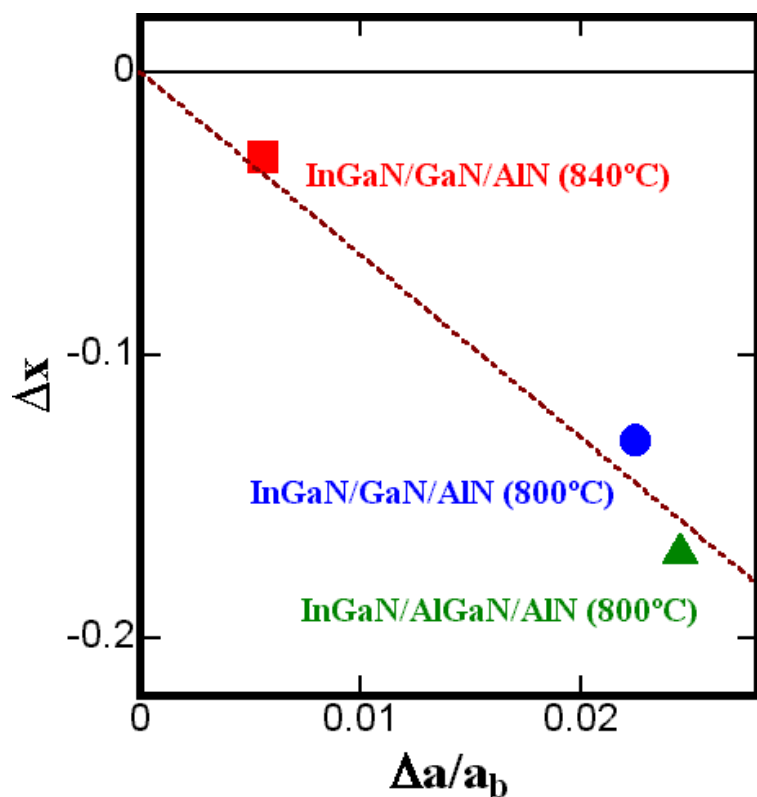


**Figure 6.** The composition pulling,  $\Delta x$ , in the initial growth stage of InGaN on the GaN and AlGaN epitaxial layers as a function of lattice mismatch  $\Delta a/a_b$ , where  $\Delta a = a_e - a_b$ ,  $a_e$  and  $a_b$  are the lattice constant of thick InGaN grown under the equilibrium condition and that of the bottom epitaxial layer (GaN or AlGaN), and  $\Delta x = x_e - x_i$ ,  $x_i$  and  $x_e$  are the indium mole fractions of InGaN grown at the initial stage and at the subsequent stage under the equilibrium condition.

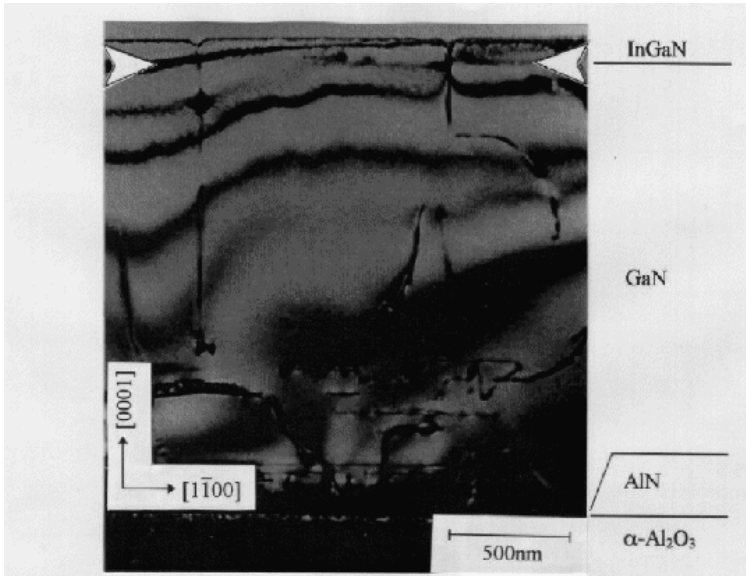


**Figure 7.** Cross-sectional TEM image of InGaN grown on GaN at 800°C for 5 min which shows the whole image of InGaN/GaN/AlN/ $\alpha$ -Al<sub>2</sub>O<sub>3</sub>.

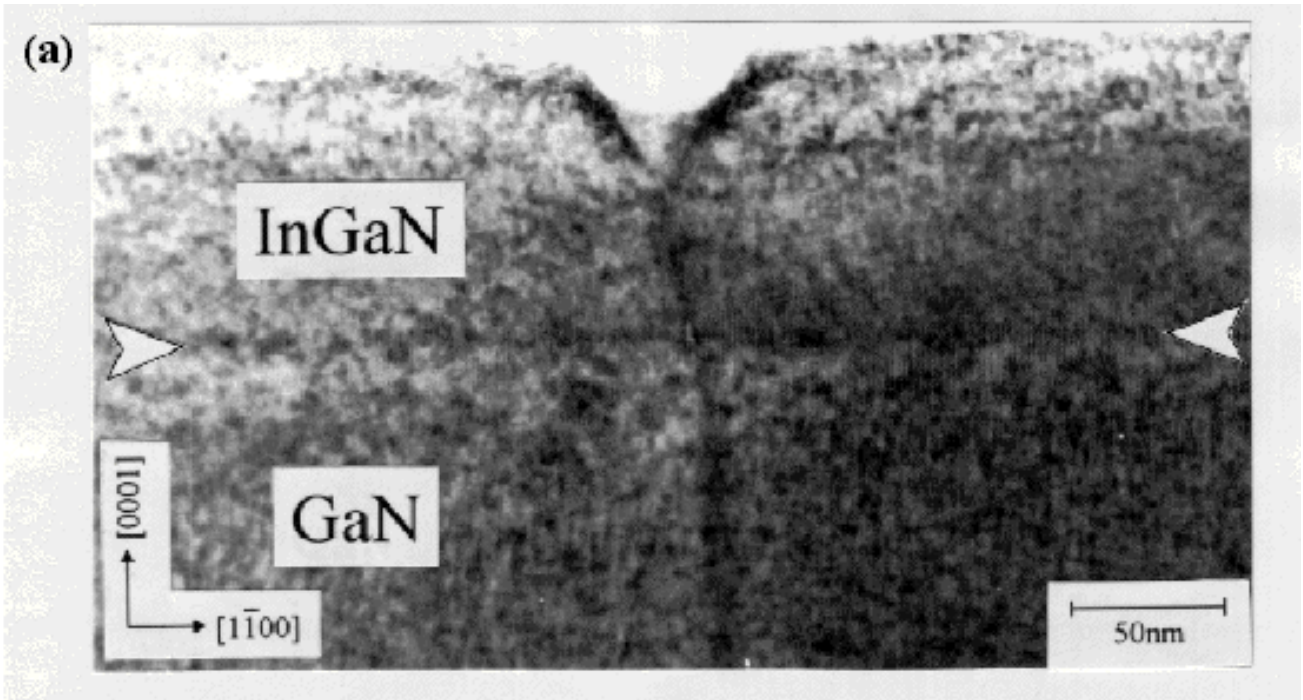


**Figure 8a.** Cross-sectional TEM image near the interface of InGaN grown on GaN at 800°C for 5 min.

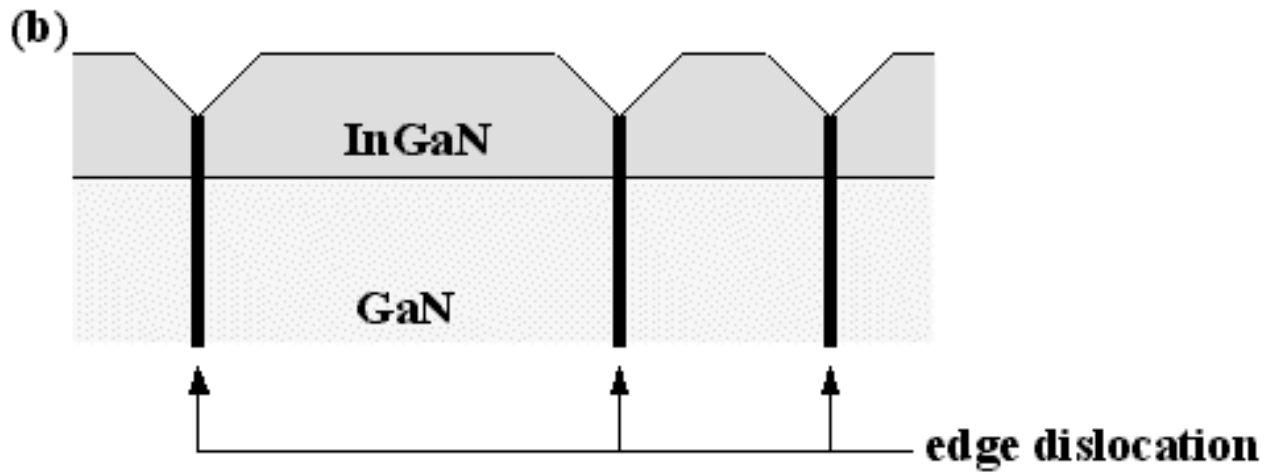


**Figure 8b.** Schematic diagram of InGaN grown on GaN at 800°C for 5 min.

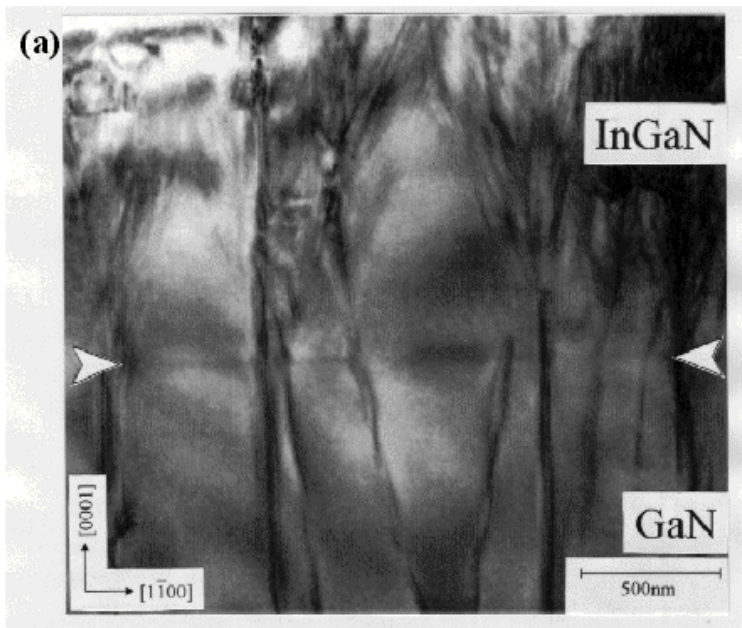


**Figure 9a.** Cross-sectional TEM image near the interface of InGaN grown on GaN at 800°C for 60 min.

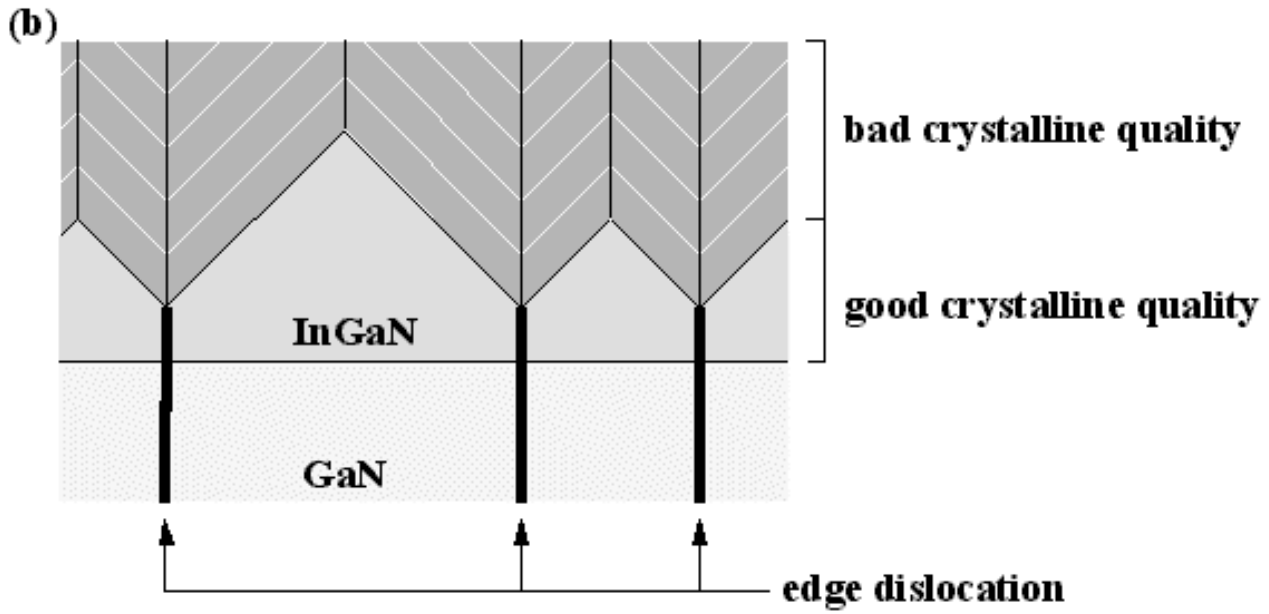


**Figure 9b.** Schematic diagram of cross-sectional images of InGaN grown on GaN at 800°C.

© 1997 The Materials Research Society